Bull. Soc. R. Sci. Liège, 2024, **93**(2), 572–581 *Peer-reviewed conference paper*
doi:10.25518/0037-9565.11800

A Study of Ultracompact H II Regions with Extended Emission: their Importance, Origin, and Evolution

Jyotirmoy DEY[1,*], Jagadheep D. PANDIAN[1], Dharam LAL[2], Michael RUGEL[3], Andreas BRUNTHALER[3], Karl MENTEN[3], Friedrich WYROWSKI[3], Nirupam ROY[5], Sergio DZIB[3], Sac-Nicté X. MEDINA[3,4] and Sarwar KHAN[3]

[1] Department of Earth and Space Sciences, Indian Institute of Space Science and Technology, Trivandrum, Kerala 695547, India
[2] National Centre for Radio Astrophysics–Tata Institute of Fundamental Research, Post Box 3, Ganeshkhind P.O., Pune 411007, India
[3] Max Planck Institute for Radioastronomy (MPIfR), Auf dem Hügel 69, 53121 Bonn, Germany
[4] German Aerospace Center, Scientific Information, 51147 Cologne, Germany
[5] Department of Physics, Indian Institute of Science, Bengaluru 560012, India
[*] Corresponding author: dey.jyotirmoy04@gmail.com

Paper presented at the 3rd BINA Workshop on "Scientific Potential of the Indo-Belgian Cooperation", held at the Graphic Era Hill University, Bhimtal (India), 22nd–24th March 2023.

Abstract

Studies of ultracompact H II regions have shown that the Lyman-continuum photon (hereafter, Ly-photon) rates inferred from the radio emission and values based on the infrared emission are inconsistent with a rate estimated from radio being up to 90% lower. One possible solution to this inconsistency is the presence of extended radio emission associated with the ultracompact core, which is undetected by most interferometric arrays, due to the lack of very short baselines. Since such extended emission would require a significantly higher rate of Ly-photons to keep its ionization state compared to the compact core, its existence would also resolve the "age problem of the ultracompact H II regions: the number of ultracompact H II regions observed in the Galaxy is much larger than what is expected based on their dynamical age (sound crossing time)," as there is no need to confine the ionized gas within the ultracompact core. To test this hypothesis, we conducted a study of eight ultracompact H II regions with extended emission using radio data from the *upgraded Giant Metrewave Radio Telescope* (1.25–1.45 GHz) and the GLOSTAR survey (4–8 GHz), and infrared data from the UKIDSS, 2MASS, MIPSGAL, and Hi-GAL surveys. From our study, we found that the Ly-photon rate inferred from the radio emission is consistent with that inferred from the total infrared luminosity to within 20–30% when we include the extended emission. Furthermore, we identified the candidate ionizing stars and observed that, in some cases, multiple stars were responsible for ionizing the neutral gas in an ultracompact H II region. Here, we present the key results for one region (G19.68–0.13) out of the entire list of our targets.

Keywords: ultracompact H II regions, Lyman-continuum photon, dust emission, radio observation.

1. The Ultracompact H II Region and High-mass Star Formation

Massive stars ($M \geq 8\,M_{\odot}$) produce enough UV photons to ionize the neutral gas surrounding them, producing H II regions that are bright at radio and infrared wavelengths. The H II regions are seen in different morphologies, such as spherical, cometary, core-halo, shell, and irregular (Wood and Churchwell, 1989; Motte et al., 2018), which occur due to reasons such as the motion of the star through the natal molecular cloud, density gradient in the environment, the temperature gradient of the gas, etc. H II regions are classified based on their size and electron density, with regions with sizes ≤ 0.1 pc and densities $\geq 10^4\,\mathrm{cm}^{-3}$ being called ultracompact H II regions (UCHRs; Wood and Churchwell 1989; Kim and Koo 2001). Wood and Churchwell (1989) and Kurtz et al. (1994) noted that the Ly-photon rate inferred from the radio continuum emission of UCHRs was significantly lower ($\sim 90\%$) than that inferred from far infrared fluxes measured by IRAS. This was suggested to be due to the absorption of Ly-photons by a large amount of dust in the H II region. An alternate explanation for the missing Ly-photons is the presence of extended radio emission surrounding the UCHRs at their center. Such an extended emission associated with the central ultracompact (UC) core (or H II region) requires 10 to 20 times more Ly-photons to maintain its ionization compared to the UC core alone (Kurtz et al., 1999; Kim and Koo, 2001; de la Fuente et al., 2020). Since the extent of diffuse emission is often underestimated on account of the lack of sensitivity of interferometers to large angular scales, the Ly-photon rate from radio emission may be significantly underestimated. We have studied eight UCHRs with extended emission at radio and infrared wavelengths to explore the importance of extended emission. Here, the results for one region are showcased that has similar morphological properties (e.g., the extended emission surrounding the UC core as seen in the radio observations) to the rest of the targets.

2. Observations and Data Analysis

We observed the target H II regions using the *upgraded Giant Metrewave Radio Telescope* (uGMRT; Swarup 1990; Gupta 2014) with the GWB correlator as the backend. The receiver was configured to have a bandwidth of 200 MHz centered at 1350 MHz with 8192 channels (BAND–5). The uGMRT has a native angular resolution of $\sim 2''$ and is capable of detecting angular scales up to $7'$ in BAND–5. We used the radio sources 3C48 and 3C286 as the flux density and bandpass calibrators according to their availability, whereas 1822–096 was used as the gain calibrator, which has a flux of 5.6 Jy in this band. The data were analyzed by using the NRAO *Common Astronomy Software Applications* (CASA 5.7; McMullin et al. 2007) package. In addition to the radio continuum, a total of four (H167α to H170α) radio recombination lines (RRL) were observed towards our target UCHRs to study the velocity distribution of the ionized gas.

Besides the radio data from the uGMRT, we have also used data from the *global view on star formation* (GLOSTAR; Medina et al. 2019; Brunthaler et al. 2021) Galactic plane survey. The GLOSTAR survey was carried out with the *Karl G. Jansky Very Large Array* (VLA) in the most compact D-configuration and more extended B-configuration (for this work, we are using data from the D-configuration) covering seven RRLs, and the continuum emission in

full polarization within 4–8 GHz. The detected RRLs from both uGMRT and GLOSTAR are stacked, leading to an increment in the signal-to-noise ratio by a factor of ≈ 2. The stacked RRL maps from these two surveys have a velocity resolution of $5\,\mathrm{km\,s^{-1}}$ and an angular resolution of $25''$.

To construct a spectral energy distribution (SED) of the UCHRs at infrared wavelengths, we have used data from the *Spitzer* GLIMPSE (3.6 μm, 4.5 μm, 5.8 μm, and 8.0 μm; Churchwell et al. 2009), *Spitzer* MIPSGAL (24 μm; Carey et al. 2009), and HiGAL (70 μm, 160 μm, 250 μm, 350 μm, and 500 μm; Molinari et al. 2010) surveys. Before constructing the SED, the mid-infrared images were processed using the MOsaicker and Point source EXtractor (MOPEX; Makovoz and Marleau 2005) package to eliminate the point sources and estimate the total flux, including the extended emission.

The Ly-photon rate is calculated from the observed radio continuum flux, from which the spectral type of the parent star is also estimated if a single zero-age main sequence star (ZAMS) was responsible for ionizing the entire region. Next, we constructed color-magnitude and color-color diagrams using the near-infrared point source catalogs from the 2MASS (Skrutskie et al., 2006) and UKIDSS-GPS (Lawrence et al., 2007) surveys to identify the candidate ionizing stars accounting for the Ly-photon rate observed in the radio observations. The SED of dust was modeled to determine the total infrared luminosity, which allows one to estimate the fraction of photons absorbed by the dust. These steps were repeated for the individual sources, and in the following section, we present the results for one of the targeted H II regions to demonstrate the significance of extended emission in resolving the mismatch between the Ly-photon rates.

3. Results for the UCHR G19.68–0.13

The UCHR G19.68–0.13, a core-halo type according to Wood and Churchwell (1989), is located at a kinematic distance of 11.7 kpc with $V_{\mathrm{LSR}} = 56.9\,\mathrm{km\,s^{-1}}$ (Urquhart et al., 2018). We measured the flux inside the 3σ-level contours, and it's estimated to be 0.622 ± 0.012 Jy using uGMRT at 1.35 GHz (left panel of Fig. 1), and 0.481 ± 0.018 Jy at 5.8 GHz from the GLOSTAR survey (right panel of Fig. 1—taken from Medina et al., in prep.). The in-band spectral index (α) from the GLOSTAR survey is -0.098 ± 0.006, which indicates that the emission is optically thin in the 4–8 GHz regime. The value of the spectral index is broadly consistent with the uGMRT flux showing that the emission is optically thin down to 1.35 GHz. The Ly-photon rate is calculated using the following equation (Mezger and Henderson, 1967; Schmiedeke et al., 2016),

$$N_{\mathrm{Ly}} = 4.76 \times 10^{42}\ \nu^{0.1}\ d^2\ S_\nu\ {T_{\mathrm{e}}}^{-0.45}$$

where S_ν is the flux density in Jy, ν is the frequency in GHz, d is the distance to the source in parsec (pc), and T_{e} is the electron temperature of the ionized gas ($T_{\mathrm{e}} = 10^4$ K, typical for a galactic H II region). For G19.68–0.13, the Ly-photon rate is estimated to be, $\log N_{\mathrm{Ly}} = 48.80$ and 48.77 for uGMRT and GLOSTAR, respectively. So, if a single ZAMS star was responsible for ionizing the entire region, it would be of spectral type O6.5 or earlier (Martins et al., 2005). Based on the analysis of near-infrared data, we detected five candidate stars (Fig. 2) with a total

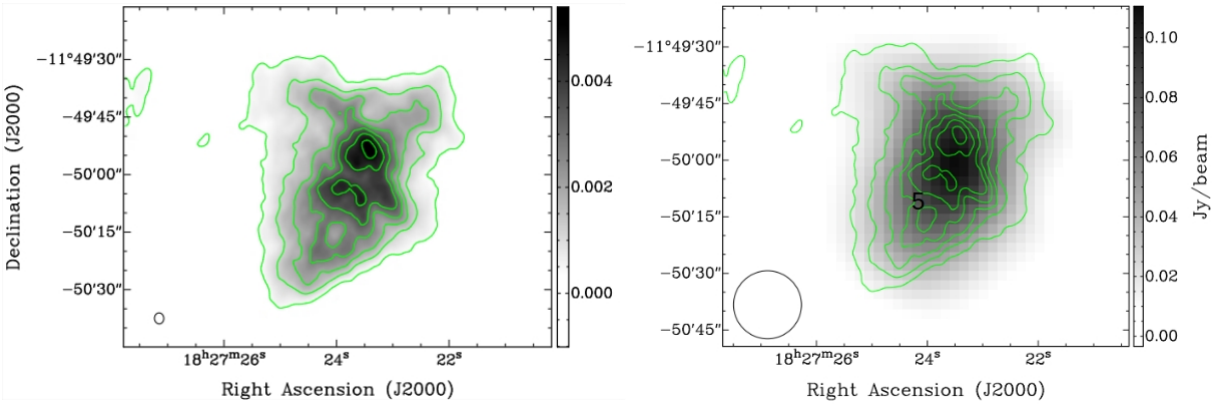

Figure 1: (left) The uGMRT radio continuum image of G19.68–0.13 at 1.35 GHz with $\sigma = 60\,\mu$Jy beam^{-1}. The $2''$ beam is shown at the bottom left corner of the figure. The contours start at the 3σ-level of 0.18 mJy beam^{-1} and increase in steps of 0.75 mJy beam^{-1} thereafter. (right) The GLOSTAR radio continuum image of G19.68–0.13 at 5.8 GHz with $\sigma = 200\,\mu$Jy beam^{-1}. The $18''$ beam is shown at the bottom left corner of the figure. The overlaid radio contours are identical to those of the left panel.

Ly-photon rate ($\log N_{\rm Ly}$) between 48.21 and 48.85, which is sufficient to explain the ionization of the H II region inferred from radio wavelengths.

Next, we studied the peak velocity distribution of the ionized gas (Fig. 3) across G19.68–0.13 using RRL observations from uGMRT and GLOSTAR and found that the distribution is smooth and continuous (without any abrupt changes in its value) across the extended emission with a small gradient from the north-west to south-east direction (52–58 km s^{-1}; shown using a magenta line in Fig. 3). A similar velocity gradient (54–59 km s^{-1}) is also discovered using the data from the ^{12}*CO (3–2) High-Resolution Survey* (COHRS; Dempsey et al. 2013) of the molecular gas. This suggests that the extended emission has originated from the candidate ionizing stars that formed within the same molecular cloud and is not a relic from an earlier generation of star formation. The latter would have resulted in a discontinuity in the velocity of ionized gas as one goes from the extended emission to the UC core (Garay et al., 1998; Kurtz et al., 1999).

To compute the total luminosity from dust emission, the infrared SED (Fig. 4) of the H II region from 500 μm to 3.6 μm was then modeled using the DustEM package (Compiègne et al., 2011). (Check https://www.ias.u-psud.fr/DUSTEM/userguide.html for more details.) The DustEM is a numerical tool that computes the SED of dust emission after taking into account the effects of extinction, re-emission, etc. The main input parameters and keywords include grain type, size distribution, optical properties and heat capacities of grain, etc. In this work, we have used a dust model comprising polycyclic aromatic hydrocarbons, amorphous carbons, and amorphous silicates with size distribution and physical properties as defined in Compiègne et al. (2011). Since infrared emission is a result of emission from the central stars that are reprocessed by dust, one can use the luminosity of dust emission to estimate the total Ly-photon

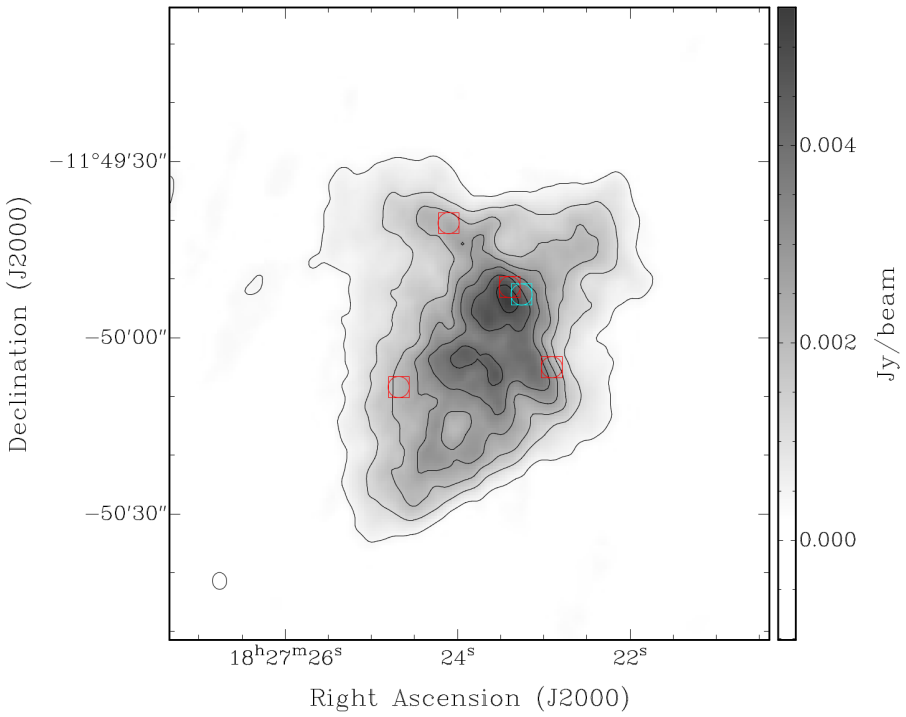

Figure 2: The candidate ionizing stars observed towards G19.68–0.13 using 2MASS and UKIDSS surveys. The star in cyan is of spectral type O9 or earlier, and the other stars are between B3 and O9. Altogether, the total Ly-photon contribution ($\log N_{\rm Ly}$) from these stars is $48.21 \leq \log N_{\rm Ly} \leq 48.85$.

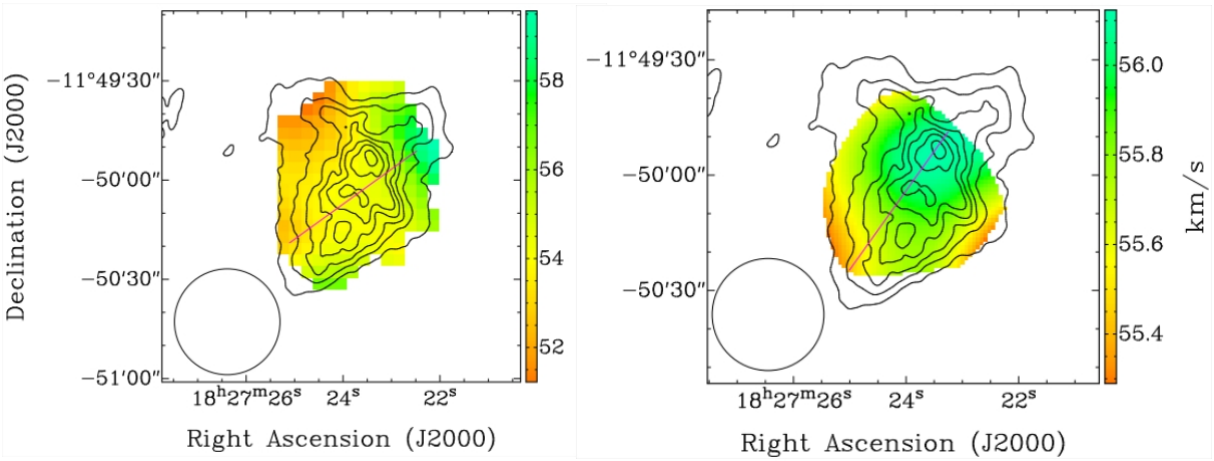

Figure 3: The peak velocity distribution maps of the ionized gas observed using GLOSTAR (left) and uGMRT (right) at 25″ resolution. The beam sizes are shown at the bottom left corner of the respective figures. The overlaid radio contours are identical to those of Fig. 1.

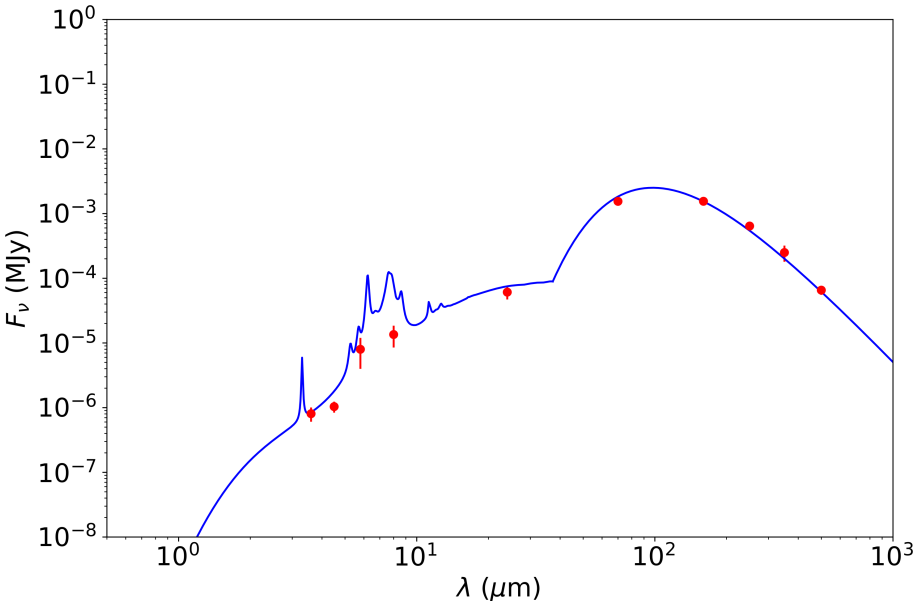

Figure 4: The figure shows the fit to the infrared SED of G19.68–0.13 obtained using the DustEM package.

rate. Then, the fraction (f) of Ly-photons contributing to hydrogen ionization can be estimated using the following equation (Inoue et al., 2001),

$$\frac{L_{\rm IR}^{\rm dust}(8-1000\,\mu m)/L_\odot}{N_{\rm Ly}/5.63\times10^{43}\,{\rm s}^{-1}} = \frac{1-0.28\,f}{f}, \tag{1}$$

where $L_{\rm IR}^{\rm dust}$ is the integrated infrared luminosity between 8–1000 μm. We have estimated $f \approx 0.78$ for G19.68–0.13, meaning 78% of the intrinsic Ly-photons produced by the ionizing stars are *not* absorbed by the dust and contribute to maintaining the ionization of the H II region. Our estimation of f indicates that the fraction of Ly-photons absorbed by the dust is roughly 20% (compared to $\sim$ 90% before; Kurtz et al. 1994). Thus the detection of extended emission surrounding the UC core significantly reduces the requirement of a large amount of dust proposed in the earlier studies and provides an explanation for the Ly-photons that were missing in the combined studies using the radio and infrared wavelengths. In their studies, Kim and Koo (2001), Ellingsen et al. (2005), and de la Fuente et al. (2020) also obtained similar results. Thus, our ongoing study, in combination with theirs, provides further evidence for the role of extended emission in explaining the missing Ly-photons.

4. Conclusions

We have presented radio and infrared observations of the H II region G19.68–0.13 using data from the uGMRT and GLOSTAR surveys. Our analysis suggests that the ionizing star (if a single ZAMS object) responsible for ionizing the H II region is of spectral type O6.5 or earlier, and we have identified five candidate stars from near-infrared catalogs that can cumulatively produce the observed Ly-photon rate.

Our study also provides insights into the dust absorption properties in the region. We have

estimated that roughly 20% (20–30% based on the complete sample) of the Ly-photons produced by the ionizing stars are absorbed by dust in the H II region. Thus, the extended emission plays a significant role in resolving the mismatch between the Ly-photon rates obtained from radio and infrared observations.

Our findings emphasize the need for more extensive radio and infrared observations to better understand the complex processes associated with the H II regions. The combination of these observations can provide a more comprehensive understanding of the physical properties of these regions and the underlying star-forming processes.

Acknowledgments

J. D. and J. D. P. thank the Max-Planck Society for funding this research through the Max Planck partner group initiative. D. V. L. acknowledges the support of the Department of Atomic Energy, Government of India, under project no. 12-R&D-TFR-5.02-0700. We thank the staff of the uGMRT that made these observations possible. uGMRT is run by the National Centre for Radio Astrophysics of the Tata Institute of Fundamental Research. The VLA is run by the National Radio Astronomy Observatory, a facility of the National Science Foundation operated under a cooperative agreement by Associated Universities, Inc. This work (partially) uses information from the GLOSTAR database at http://glostar.mpifr-bonn.mpg.de supported by the MPIfR, Bonn. J. D. also thanks Dr. Jean-Baptiste Jolly from the Max-Planck-Institute for Extraterrestrial Physics, and the Nordic ALMA Regional Center node for providing the Line-Stacker package. This research has made use of the SIMBAD database, operated at CDS, Strasbourg, France. This research has also utilized NASA's Astrophysics Data System, CDS's VizieR catalog access tool, and calibrated infrared images from the Spitzer Heritage Archive and Herschel Science Archive. This work was presented at the 3rd Belgo-Indian Network for Astronomy and Astrophysics (BINA) workshop. J. D. is thankful to the BINA project for providing the local support to attend the workshop.

Further Information

Authors' ORCID identifiers

0000-0003-4074-4365 (Jyotirmoy DEY)
0000-0003-4031-1121 (Jagadheep D. PANDIAN)
0000-0001-5470-305X (Dharam LAL)
0009-0009-0025-9286 (Michael RUGEL)
0000-0003-4468-761X (Andreas BRUNTHALER)
0000-0001-6459-0669 (Karl MENTEN)
0000-0003-4516-3981 (Friedrich WYROWSKI)
0000-0001-9829-7727 (Nirupam ROY)
0000-0001-6010-6200 (Sergio DZIB)

0000-0003-2580-4796 (Sac-Nicté X. MEDINA)
0000-0002-0152-9390 (Sarwar KHAN)

Author contributions

JD, JDP, and DVL were involved in uGMRT observations and data analysis; AB, KMM, MRR, FW, JDP, NR, SAD, SNXM, and SK are involved with the GLOSTAR survey. All the authors contributed to the interpretation of the results and writing the paper.

Conflicts of interest

The authors declare no conflict of interest.

References

Brunthaler, A., Menten, K. M., Dzib, S. A., Cotton, W. D., Wyrowski, F., Dokara, R., Gong, Y., Medina, S. N. X., Müller, P., Nguyen, H., Ortiz-León, G. N., Reich, W., Rugel, M. R., Urquhart, J. S., Winkel, B., Yang, A. Y., Beuther, H., Billington, S., Carrasco-Gonzalez, C., Csengeri, T., Murugeshan, C., Pandian, J. D. and Roy, N. (2021) A global view on star formation: The GLOSTAR Galactic plane survey. I. Overview and first results for the galactic longitude range $28^\circ < l < 36^\circ$. A&A, 651, A85. https://doi.org/10.1051/0004-6361/202039856.

Carey, S. J., Noriega-Crespo, A., Mizuno, D. R., Shenoy, S., Paladini, R., Kraemer, K. E., Price, S. D., Flagey, N., Ryan, E., Ingalls, J. G., Kuchar, T. A., Pinheiro Gonçalves, D., Indebetouw, R., Billot, N., Marleau, F. R., Padgett, D. L., Rebull, L. M., Bressert, E., Ali, B., Molinari, S., Martin, P. G., Berriman, G. B., Boulanger, F., Latter, W. B., Miville-Deschenes, M. A., Shipman, R. and Testi, L. (2009) MIPSGAL: A survey of the inner Galactic plane at 24 and 70 μm. PASP, 121(875), 76–97. https://doi.org/10.1086/596581.

Churchwell, E., Babler, B. L., Meade, M. R., Whitney, B. A., Benjamin, R., Indebetouw, R., Cyganowski, C., Robitaille, T. P., Povich, M., Watson, C. and Bracker, S. (2009) The *Spitzer*/GLIMPSE surveys: A new view of the Milky Way. PASP, 121(877), 213–230. https://doi.org/10.1086/597811.

Compiègne, M., Verstraete, L., Jones, A., Bernard, J. P., Boulanger, F., Flagey, N., Le Bourlot, J., Paradis, D. and Ysard, N. (2011) The global dust SED: tracing the nature and evolution of dust with DustEM. A&A, 525, A103. https://doi.org/10.1051/0004-6361/201015292.

de la Fuente, E., Porras, A., Trinidad, M. A., Kurtz, S. E., Kemp, S. N., Tafoya, D., Franco, J. and Rodríguez-Rico, C. (2020) Ultracompact H II regions with extended emission: the complete view. MNRAS, 492(1), 895–914. https://doi.org/10.1093/mnras/stz3482.

Dempsey, J. T., Thomas, H. S. and Currie, M. J. (2013) CO (3 – 2) high-resolution survey of the Galactic plane: R1. ApJS, 209(1), 8. https://doi.org/10.1088/0067-0049/209/1/8.

Ellingsen, S. P., Shabala, S. S. and Kurtz, S. E. (2005) Extended emission associated with young HII regions. MNRAS, 357(3), 1003–1012. https://doi.org/10.1111/j.1365-2966.2005.08716.x.

Garay, G., Moran, J. M., Rodríguez, L. F. and Reid, M. J. (1998) The G19.6-0.2 region of star formation: Molecular and ionized environs. ApJ, 492(2), 635–649. https://doi.org/10.1086/305046.

Gupta, Y. (2014) The GMRT: current status and upgrade plans. ASInC, 13, 441–447.

Inoue, A. K., Hirashita, H. and Kamaya, H. (2001) Effect of dust extinction on estimating the star formation rate of galaxies: Lyman continuum extinction. ApJ, 555(2), 613–624. https://doi.org/10.1086/321499.

Kim, K.-T. and Koo, B.-C. (2001) Radio continuum and recombination line study of ultracompact H II regions with extended envelopes. ApJ, 549(2), 979–996. https://doi.org/10.1086/319447.

Kurtz, S., Churchwell, E. and Wood, D. O. S. (1994) Ultracompact H II regions. II. New high-resolution radio images. ApJS, 91, 659. https://doi.org/10.1086/191952.

Kurtz, S. E., Watson, A. M., Hofner, P. and Otte, B. (1999) Ultracompact H II regions with extended radio-continuum emission. ApJ, 514(1), 232–248. https://doi.org/10.1086/306928.

Lawrence, A., Warren, S. J., Almaini, O., Edge, A. C., Hambly, N. C., Jameson, R. F., Lucas, P., Casali, M., Adamson, A., Dye, S., Emerson, J. P., Foucaud, S., Hewett, P., Hirst, P., Hodgkin, S. T., Irwin, M. J., Lodieu, N., McMahon, R. G., Simpson, C., Smail, I., Mortlock, D. and Folger, M. (2007) The UKIRT Infrared Deep Sky Survey (UKIDSS). MNRAS, 379(4), 1599–1617. https://doi.org/10.1111/j.1365-2966.2007.12040.x.

Makovoz, D. and Marleau, F. R. (2005) Point-source extraction with MOPEX. PASP, 117(836), 1113–1128. https://doi.org/10.1086/432977.

Martins, F., Schaerer, D. and Hillier, D. J. (2005) A new calibration of stellar parameters of Galactic O stars. A&A, 436(3), 1049–1065. https://doi.org/10.1051/0004-6361:20042386.

McMullin, J. P., Waters, B., Schiebel, D., Young, W. and Golap, K. (2007) CASA architecture and applications. In Astronomical Data Analysis Software and Systems XVI, edited by Shaw, R. A., Hill, F. and Bell, D. J., vol. 376 of *ASPC*, pp. 127–130. http://aspbooks.org/custom/publications/paper/376-0127.html.

Medina, S. N. X., Urquhart, J. S., Dzib, S. A., Brunthaler, A., Cotton, B., Menten, K. M., Wyrowski, F., Beuther, H., Billington, S. J., Carrasco-Gonzalez, C., Csengeri, T., Gong, Y., Hofner, P., Nguyen, H., Ortiz-León, G. N., Ott, J., Pandian, J. D., Roy, N., Sarkar, E., Wang, Y. and Winkel, B. (2019) GLOSTAR: Radio source catalog I. $28^\circ < \ell < 36^\circ$ and $|b| < 1^\circ$. A&A, 627, A175. https://doi.org/10.1051/0004-6361/201935249.

Mezger, P. G. and Henderson, A. P. (1967) Galactic H II regions. I. Observations of their continuum radiation at the frequency 5 GHz. ApJ, 147, 471–489. https://doi.org/10.1086/149030.

Molinari, S., Swinyard, B. and Other Co-authors (2010) Hi-GAL: The Herschel infrared Galactic Plane Survey. PASP, 122(889), 314–325. https://doi.org/10.1086/651314.

Motte, F., Bontemps, S. and Louvet, F. (2018) High-mass star and massive cluster formation in the Milky Way. ARA&A, 56, 41–82. https://doi.org/10.1146/annurev-astro-091916-055235.

Schmiedeke, A., Schilke, P., Möller, T., Sánchez-Monge, Á., Bergin, E., Comito, C., Csengeri, T., Lis, D. C., Molinari, S., Qin, S. L. and Rolffs, R. (2016) The physical and chemical structure of Sagittarius B2. I. Three-dimensional thermal dust and free-free continuum modeling on 100 au to 45 pc scales. A&A, 588, A143. https://doi.org/10.1051/0004-6361/201527311.

Skrutskie, M. F., Cutri, R. M., Stiening, R., Weinberg, M. D., Schneider, S., Carpenter, J. M., Beichman, C., Capps, R., Chester, T., Elias, J., Huchra, J., Liebert, J., Lonsdale, C., Monet, D. G., Price, S., Seitzer, P., Jarrett, T., Kirkpatrick, J. D., Gizis, J. E., Howard, E., Evans, T., Fowler, J., Fullmer, L., Hurt, R., Light, R., Kopan, E. L., Marsh, K. A., McCallon, H. L., Tam, R., Van Dyk, S. and Wheelock, S. (2006) The Two Micron All Sky Survey (2MASS). AJ, 131(2), 1163–1183. https://doi.org/10.1086/498708.

Swarup, G. (1990) Giant metrewave radio telescope (GMRT) – Scientific objectives and design aspects. IJRSP, 19(5&6), 493–505.

Urquhart, J. S., König, C., Giannetti, A., Leurini, S., Moore, T. J. T., Eden, D. J., Pillai, T., Thompson, M. A., Braiding, C., Burton, M. G., Csengeri, T., Dempsey, J. T., Figura, C., Froebrich, D., Menten, K. M., Schuller, F., Smith, M. D. and Wyrowski, F. (2018) ATLASGAL – properties of a complete sample of Galactic clumps. MNRAS, 473(1), 1059–1102. https://doi.org/10.1093/mnras/stx2258.

Wood, D. O. S. and Churchwell, E. (1989) The morphologies and physical properties of ultracompact H II regions. ApJS, 69, 831. https://doi.org/10.1086/191329.